Electromechanical de-icing of rectangular aluminum plates with forced vibration generated with an amplified piezoelectric actuator

Christian Bolzmacher, Edouard Leroy

Electromechanical de-icing of rectangular aluminum plates with forced vibration generated with an amplified piezoelectric actuator

Christian Bolzmacher and Edouard Leroy

CEA, LIST, Sensorial and Ambient Interfaces Laboratory, 91191, Gif-sur-Yvette Cedex, France.

Abstract

This paper describes the feasibility of a de-icing device based on forced vibrations induced in an ice-covered rectangular aluminum plate using an amplified piezoelectric actuator. The removal of the ice layer is caused by the creation of mechanical stresses induced by relatively fast time-varying mode shapes in the very low kHz-range large enough to overcome the adhesion forces at the material/ice interface.

1. Introduction

Ice accretion on aircraft during flight can severely affect the airplane's aerodynamic performance. Supercooled droplets from clouds impacting the airplane's surfaces and freezing instantaneously can accumulate and decrease the lift generated by the airfoil. The last decades, several ice protection systems have been proposed based on thermal, chemical, and mechanical strategies or a combination of those. Electromechanical solutions may provide potential in terms of energy savings, weight reduction, and durability and therefore are well-suited for electrical aircraft. The principle of electromechanical de-icing systems is based on vibrations generated by electric actuators. The deformation generated by the actuators at the ice/substrate interface induces stress in the ice and the substrate (stress = Young's modulus x strain) causing delamination. Different frequency ranges have been addressed in literature from the low frequency range [1,2], the kilohertz range [3,4], and the megahertz range [5]. The present work addresses the very low kilohertz range using amplified piezoelectric actuators with relatively low driving voltages.

2. Electromechanical de-icing with time-varying forced vibrations

It is known from literature [6,7] that traction, bending, and torsion is lowering the interfacial adhesion between an ice layer and its substrate. The stress generated at the interface reaches the ice adherence stress, resulting in ice detachment. In this study, bending vibration modes are used for de-icing. In order to create these bending modes in the structure, i.e. a rectangular plate, piezoelectric actuators have been chosen because of their compact size – ultimately allowing them to be integrated into a leading edge of an airfoil – and relatively low power consumption at low frequencies (up to a few kHz). The capability of piezoelectric actuators to generate displacements in the kilohertz range and their responsiveness makes them a good choice for highly dynamic applications. Therefore, the de-icing system proposed in this paper uses selected resonances of the structure to remove the ice layer while care is taken that the induced vibration is not affecting the structure's integrity. The piezoelectric actuator is used to create high amplitude mode shapes with quickly varying spatial frequency in order to increase the induced stresses in the ice-structure interface to overcome the adhesive forces as well as expulsing the ice from the surface. The bending modes produce normal stress (tension and compression) as well as shear stress whose intensities are a

function of the ice thickness on the plate (see Figure 1). The ice debonds or cracks when the shear and/or normal stress reach the breaking point of the ice at the ice-substrate interface [6]. For thin ice layers the neutral axis is in the substrate and therefore the ice is subjected to tension and compression depending on the phase of the vibration. If the neutral axis is at the interface of the ice and the substrate, shear stress is maximized. For thick ice layers with the neutral axis located within the ice layer, tension and compression is acting at the same time on the ice layer. In the next chapters, optimal parameters are identified for efficient ice removal on a flat plate by means of simulation and experimental verification.

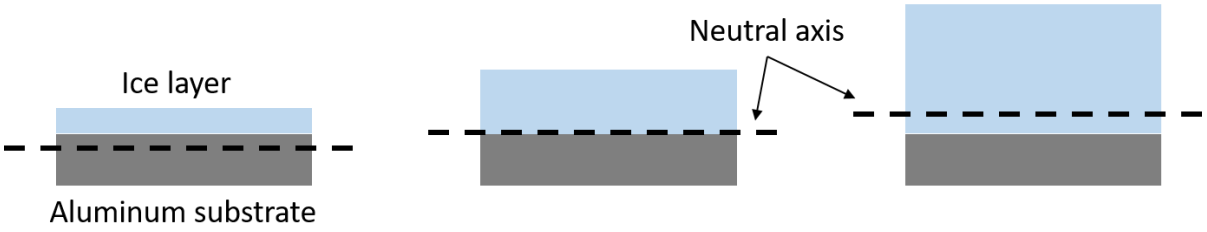

Figure 1: Neutral axis on a plate with ice layers of variable thickness [from 6].

3. Setup

The chosen test sample has been a 2024T3 aerospace grade aluminum plate of dimension 300x200x1 mm3 connected at a distance of 100 mm off-center to an APA400MML mechanically amplified piezoelectric actuator from Cedrat Technologies powered by a Cedrat LA75C amplifier (see Figure 2). The plate's dimensions have been chosen with regard to the free areas between fixations of typical general aviation airplane's leading edges. It has to be mentioned that larger dimensions favor the described approach. The APA400MML is a piezoelectric actuator designed for dynamic applications requiring high displacement amplitudes and forces at a relatively compact design (L78 mm, H24 mm, W12 mm, mass 48 g). The nominal stroke is 360 µm and the blocked-force is 180 N at a stiffness of 0.52 N/µm [8]. The actuator is screwed with a spacer to an 8 mm thick counter plate while its opposite end is glued with an aluminum disc of diameter 15 mm to the back of the plate to be de-iced. The actuator fastening is not visible from the side of the ice deposition surface and therefore does not interact with the formed ice. Several sensors (camera, accelerometer, laser vibromètre, and thermocouples) have been integrated in the set-up to measure and visualize the de-icing process. The ice has been generated in an environmental chamber at controlled temperatures depending on the type of ice to be investigated. Glaze ice (transparent or clear ice) has been created at a chamber temperature of -10°C with an atomized water injection of a duration of 15 s creating a transparent ice layer of thickness 0.3 mm. Next, the chamber temperature is returned to -10°C and then atomized water is injected again. This process is repeated until the desired ice thickness is reached. The precipitation rate is 8 ml/s and the droplet size is between 200 µm and 300 µm in diameter. A pressure of 1 bar is applied to create these droplets from liquid water. Figure 2 shows a mask used to prevent ice creation on the border of the flat plate on the vertical sides of the system, which would influence the de-icing behavior of the device. A mixed ice with a contact layer of glaze ice and then becoming rime ice (white ice) has been created at chamber temperatures of -15°C with repeated atomized water injections of 5 s.

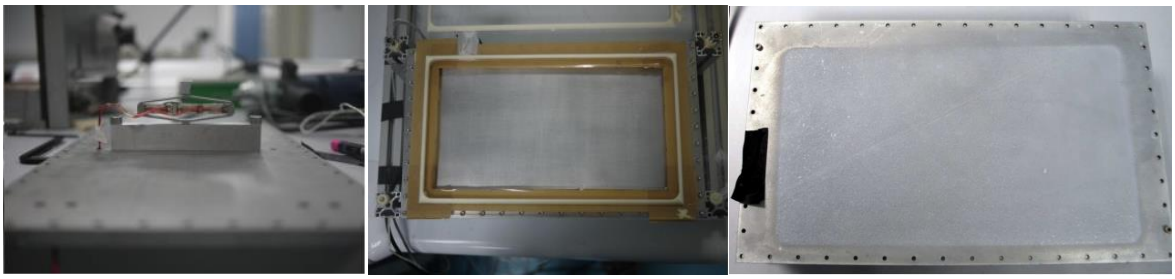

Figure 2: Setup of the de-icing system; (a) Amplified piezoelectric actuator fixed to the base structure; (b) Top view of the fixed aluminum plate with ice deposition mask; (c) Mixed ice of 0.8 mm thickness.

4. Modal behavior of the aluminum plate

Prior to the actual de-icing experiments, the plate's vibrational response has been evaluated using Finite Element Analysis (FEA) in ANSYS Workbench and laser vibrometer measurements. It has to be noted that the APA400MML actuator is sensitive to external push and pull forces exceeding 150 N [8]. That is the reason why the actuator is placed off-center at a distance of 100 mm from the center. This way the actuator is closer to the fixation, which should limit to some extent these push and pull forces compared to the center position where the vibration is geometrically less constrained.

4.1 Finite element modal and harmonic analysis

The geometry of the plate is simulated by assuming that the fixation screws are assimilated to a fixed boundary at a distance of 10 mm of the plate's borders. The actuator is modeled as providing a stiffness of 550 N/mm [8] and a mass of 1.8 g is placed at the point of attachment of the actuator. This mass corresponds to the mass-spring system formed by the actuator at no load (according to the manufacturer's data f0=2738 Hz, $m=(2*\pi*f)^2*k$). The plate material is considered to be a standard aluminium alloy (E=71 GPa, ρ=2770 kg.m-3, ν=0.33). Two studies are conducted: a modal study and a harmonic study on a modal basis, the latter allowing a direct comparison with the experimental measurements. Figure 4 shows the simulated Eigenmodes up to mode 12. The eccentric position of the actuator is slightly modifying the mode shapes but the patterns known from literature for flat rectangular plates are still recognizable.
For the harmonic analysis, a constant force excitation of 8 N over the frequency range from 100 Hz to 5 kHz has been applied to the plate at the actuator's anchor point. Figure 3 depicts the maximum vibration amplitudes at selected points on the plate.

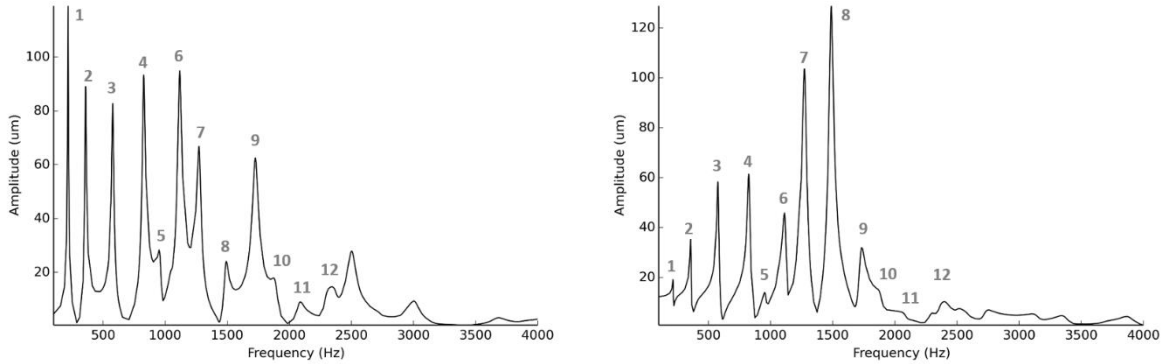

Figure 3: Simulated harmonic response of the system with a constant 8 N excitation 100 mm off-center (simulating the actuator at a position of 100 mm left of the center); On the left, simulation measured at the center point and on the right on a side point (80 mm left of the center).

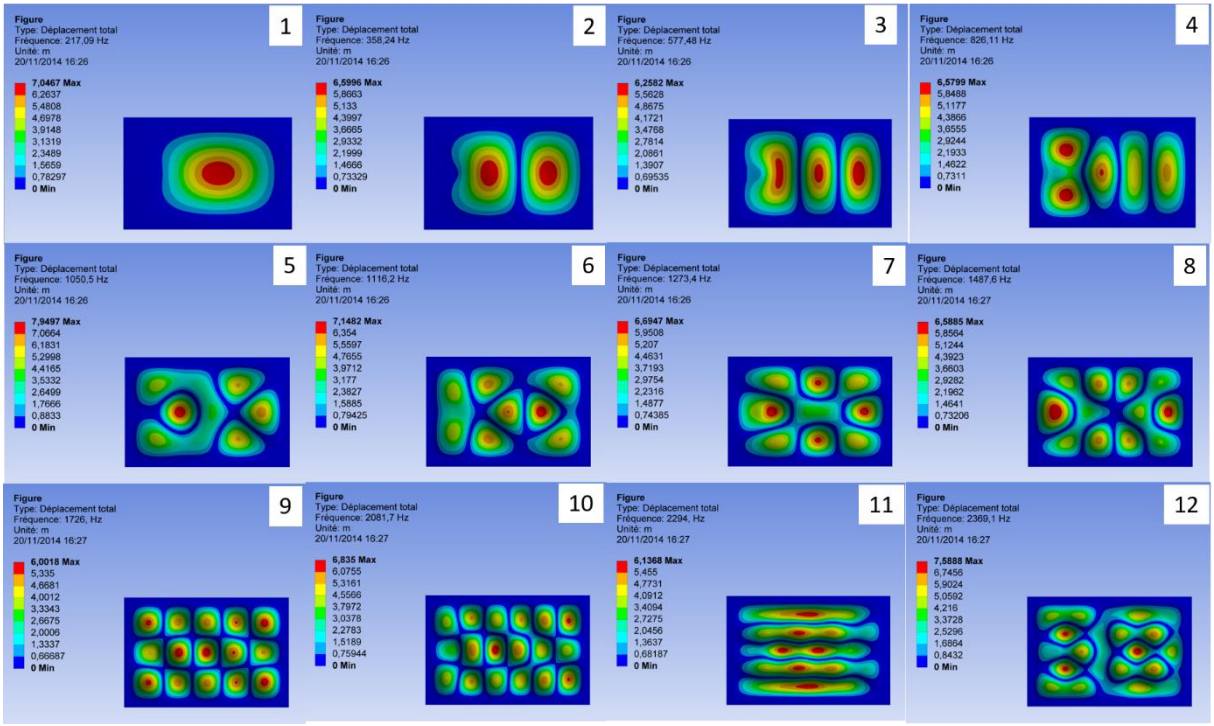

Figure 4: Simulated mode shapes of the first 12 Eigen modes of the aluminum plate with an APA400MML located 100 mm left off-center.

4.2 Experimental verification of the Eigen modes

Next, the frequency response of the device is measured. For this purpose, the plate is placed under a robotic XYZ table equipped with a POLYTEC vibrometer. The measurement of the vibration at different frequencies and different points of the plate allows to extract the harmonic response and to estimate its Eigen frequencies and Eigen modes.

In order to obtain the vibration mode shape, a total of 540 points is scanned. The frequency responses are extracted from the Fourier transforms of the response to a scan. The vibrometer measurements are normalized by the voltage applied to the actuator and the measured quantity is then expressed in m/V. The measurements are made for an amplitude of 2.5 Vpp and a logarithmic sweep between 20 Hz and 50 kHz with a duration of 0.5 s.

Figure 5 shows the frequency response of the device at the center of the plate (left) and for a point 80 mm from the center (right) measured with the laser vibrometer in a linear scale. Modes 2 and 3 show in both cases the highest vibration amplitudes. The mode 3 corresponds very likely to the actuator's first resonance located at 630 Hz in a blocked-free configuration according to the manufacturer's datasheet. The frequency shift of mode 3 located at 546 Hz might be due to the mass applied to actuator by the plate. At higher frequencies, the group of modes 6, 10, and 13 stand out for the center position. At the side position (see Figure 5 on the right), modes 7, 9, 10, and 12 show the highest vibration displacement amplitudes. The amplitude of these modes are in the range of 250 µm to 400 µm for a 40 Vp driving signal (obtained by multiplication of the measured quantity given in m/V with the driving voltage).

A vibrometer scan allows observing the mode shapes shown up to mode 12 in Figure 6. The wavelengths for these modes vary between 200 mm and 80 mm. Mode 12 is interesting because it combines a high amplitude with a relatively short wavelength in the direction of the airflow on an airfoil. This mode might be present even in a curved plate as can be found on a leading edge.

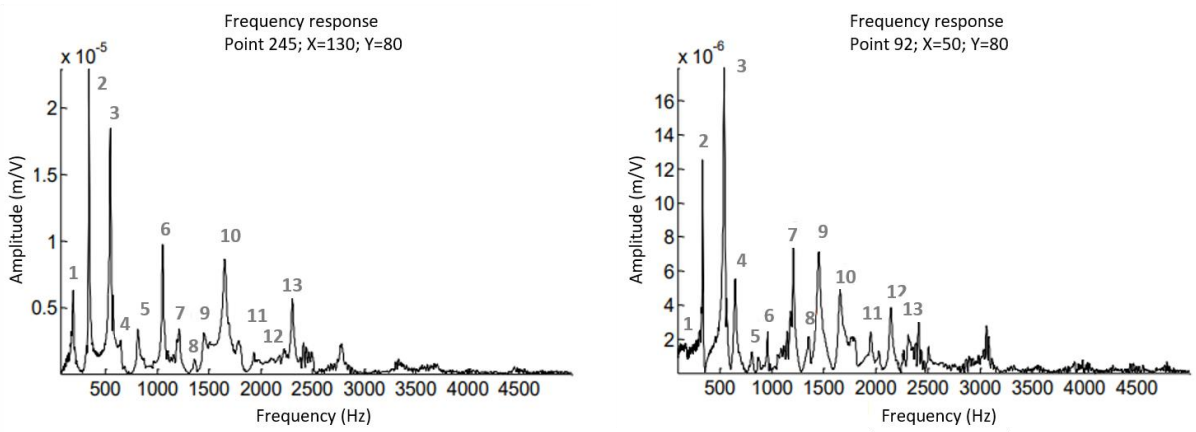

Figure 5: Harmonic response analysis of the aluminum plate measured with a laser vibrometer; (left) center point, (right) 80 mm left from the center; actuator position 100 mm left of the center.

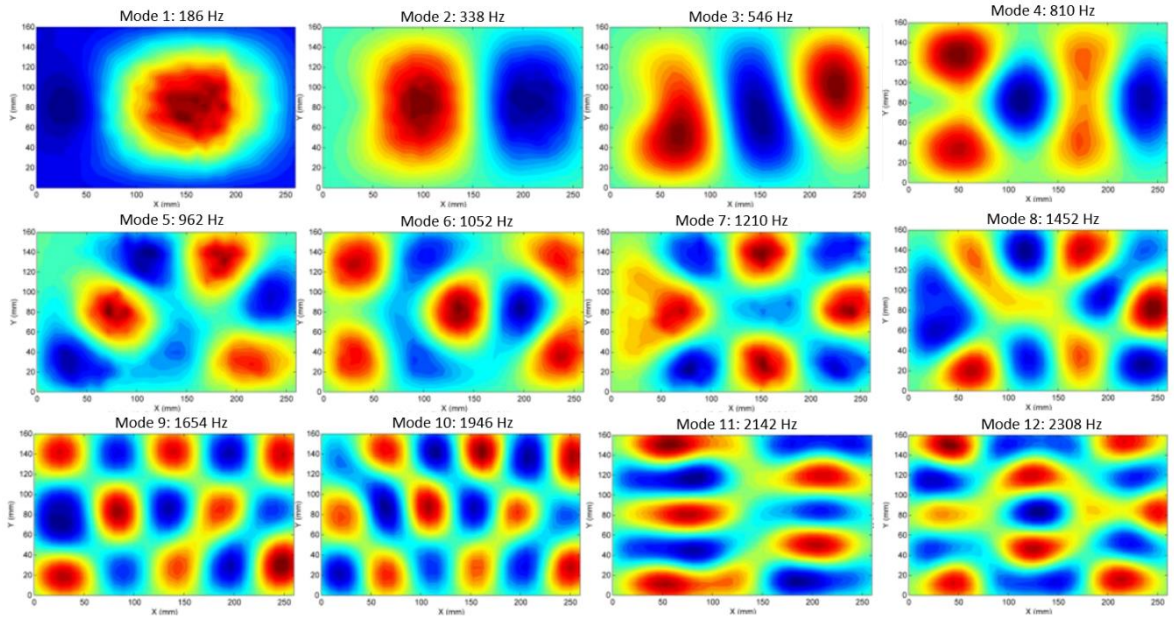

Figure 6: Laser vibrometer scans visualized as a color map in Python for the actuator fixed at a distance of 100 mm left off-center.

5. Electromechanical de-icing experimentation

This section presents the different results obtained for the de-icing tests with the above described prototype. Various parameters are investigated to optimize the de-icing performance such as the actuator's displacement amplitude by means of varying driving voltage, the applied frequency range, the vibration time, and the ice layer thickness. It has to be noted that the application of individual Eigen modes did not yield robust de-icing of the plate. That is the reason why sweep signals over selected frequency ranges have been applied.

5.1 Influence of the displacement amplitude on the de-icing performance

Two test results are presented here to show the effect of the actuator voltage on the de-icing performance of the system on a 2 mm thick glaze ice layer. For both tests a 2 s logarithmic sine sweep signal from 4 kHz (start frequency) to 100 Hz (stop frequency) has been applied to

the actuator. That is the signal presented in Figure 9 as a solid line. In the first test, a voltage of 75 Vp (with an offset of 75 V) and in the second test a voltage of 40 Vp (with an offset of 40 V) was applied to the actuator, which gives a no-load output displacement amplitude of the actuator of 360 µm and 192 µm, respectively. The frequency range has been selected based on the harmonic analysis of the aluminum plate presented in section 4.2 where only little vibration activity is present above 4 kHz due to amplifier current restrictions. In both cases a clear and complete de-icing is obtained with all ice removed on the first sweep for the 75 Vp signal whereas the 40 Vp signal requires three consecutive sweeps (0.1 s hold time) to remove most of the ice.

Two phases can be observed for the de-icing process, first the ice is detached from the surface and in a second step expulsed as shown in Figure 7. The detachment takes place for the 75 Vp signal at around 2.2 kHz and again between 2 kHz and 1.7kHz. Expulsion takes place between 800 Hz and 700 Hz with some pieces already expulsed at 1.5 kHz leading to a de-iced area of around 95 %.

For the 40 Vp signal, 5 frequency ranges have been identified. Between 2.7 kHz and 2.2 kHz the ice layer is detached from the surface and is then expulsed on frequencies around 2.1 kHz, 2 kHz, between 1.3 kHz and 1 kHz, and finally between 700 Hz and 400 Hz. No activity has been observed at lower frequencies. Three repetitions have been required to de-ice the surface by about 90 % in this case. That means a sequence of 6 seconds is done.

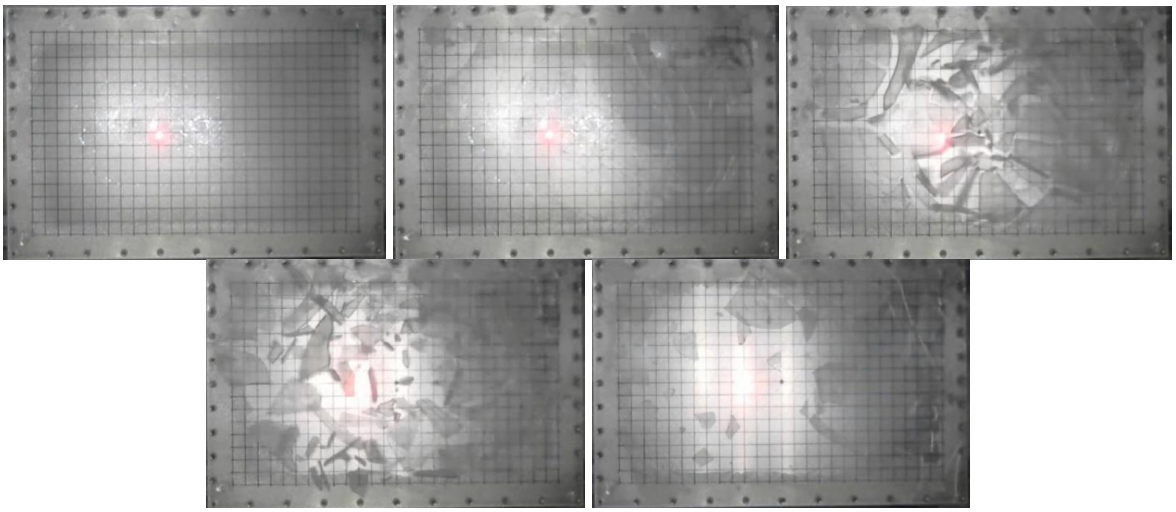

Figure 7: De-icing phase for a 75 Vp signal; upper left: before activation, center: detachment of the ice layer around 1.8 kHz, upper right: start of ice expulsion; bottom left: halfway of expulsion cycle, and bottom right: end of cycle.

5.2 Influence of the frequency on the de-icing performance

Next, the influence of the excitation frequency on a 1.2 mm thick glaze ice layer is investigated (tests 3 to 5 in Table 1). Following several damages of the actuator, one of the first changes proposed is the avoidance of the resonance zone of the actuator around 630 Hz. In order to avoid this zone, the low frequency part of the excitation signal (i.e. stop frequency) is raised from 100 Hz to 700 Hz and the drive signal is set to 40 Vp. This test can be compared to test 2 of section 5.1. As for test 2, the ice detachment starts at 2.2 kHz and is more pronounced around 1.6 kHz before being ejected around 1.5 kHz. A second expulsion step is observed between 1.4 kHz and 1.3 kHz. After the first sine sweep, more than 70% of the surface is de-iced. The second and third sweep (a total of three consecutive sweeps with a hold time

between two sweeps of 0.1 s) increase this rate to around 85% and 90%, respectively. The rise of the low frequency part of the signal from 100 Hz to 700 Hz seems to improve the de-icing by increasing the power density injected in the higher frequencies of the range 700-4000Hz (sweep time maintained at 2 s). It should be noted that the ice layer was only 1.2 mm compared to 2 mm at test 2, which is more challenging to de-ice.

Next, the effect of the high frequency is evaluated by reducing the start frequency. In order to optimize the range of frequencies in which the energy is injected, first, a sine sweep between 3 kHz and 700 Hz is used. A very clear detachment of the ice layer around 2.7 kHz and this until 2.2 kHz when the ice begins to be expelled can be observed. A first wave of expulsion around 2.1 kHz is quickly followed by a second wave around 1.8 kHz and finally a third around 1.6 kHz. The result is an ice removal of around 95 % with two consecutive sine sweeps. The reduction of the frequency range once again demonstrates its usefulness. It has been noted that the de-icing frequency bands correspond to high amplitude resonance peaks measured with the laser vibrometer (see section 4.2) and in particular to modes 7, 9, and 10 located between 1 kHz and 2 kHz. The purpose of the last test is therefore to see whether a tightening of the frequency range (1 kHz – 2.1 kHz) around these frequencies significantly improves the de-icing. Video images show a detachment around 1.7 kHz followed by expulsion phases at 1.5 kHz, 1.3 kHz, and around 1.0 kHz, respectively. This corresponds to modes 10, 9, 7, and 6, respectively.

An interesting effect related to the size of the ice fragments can be noted from these various tests. It seems that the size of the fragments is getting smaller when the high frequency part of the sine sweep is higher (see Figure 8). This phenomenon could essentially come from the pre-cracking that occurs during the take-off of the ice. This detachment can be done by a higher order mode. If the amplitude is not sufficient to expel the ice at that moment, it allows a lift-off and probably a cracking of the ice, which, due to a smaller wavelength, creates smaller fragments.

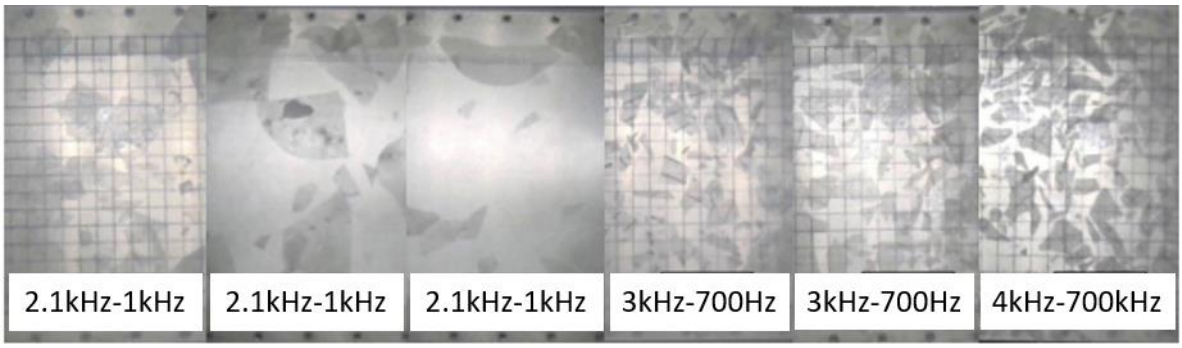

Figure 8: Fragmentation of the ice layer in small fragments depending on the excitation frequency; frequency increasing from left to right.

It can be noted that the use of a logarithmic sweep ensures a constant number of periods per frequency, thus, it favors the time spent at low frequencies. This means that the increase from 100 Hz to 700 Hz allows multiplying by two the time spent on the frequencies from 700 Hz to 4 kHz. It can reasonably be estimated that the power injected in this frequency range is then multiplied by two. The reduction of the high frequency part from 4 kHz to 3 kHz further increases the excitation time of each frequency by a factor of 1.2. Finally, setting the frequency to a band between 2.1 kHz and 1 kHz increases the excitation time by another factor of 2 as shown schematically in Figure 9.

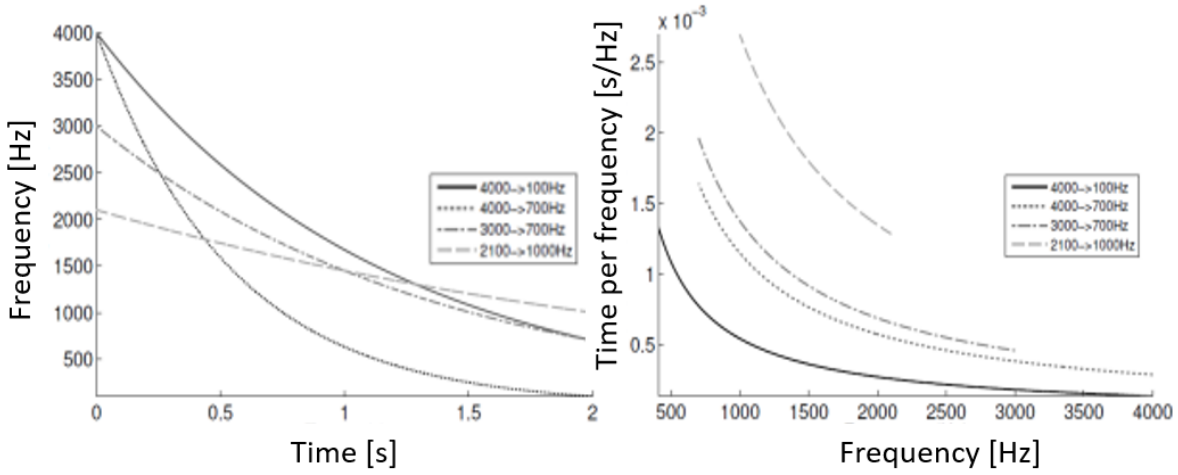

Figure 9: Effect of reducing the frequency spectrum on the time spent on each single frequency.

5.3 Ice thickness

The effectiveness of de-icing is also related to the thickness of the ice as depicted in Figure 1 with regard to the neutral axis. It can be considered that the ice is detached thanks to the stresses generated at the interface with the plate, which exceed the mechanical adhesion forces of the ice. In the described de-icing system, the ice is subjected to bending. With equal deformation introduced by the actuator, the maximum stress in the plate-ice sandwich subjected to bending is directly related to its thickness. For thin ice layers, the ice is following the deformation of the plate experiencing only small stress. If the neutral axis is located at the ice/plate interface, shear stress is highest allowing de-bonding of the ice and subsequent expulsion. When the neutral axis is within the ice layer highest stresses are applied due to amplified strain in the ice layer. It can therefore be deduced that for thicker (glaze-type) ice layers even a smaller deformation of the plate will cause its rupture and potentially its detachment. This reasoning is consistent with observations in literature [6].
Numerous tests have been conducted to estimate the limits of the technology used for de-icing. All tests carried out in the frequency range [3 kHz to 700 Hz] with a thickness greater than one millimeter have allowed a very important de-icing (> 95 %) using one or several 2 s sine sweeps. Below one millimeter, it becomes more complicated to de-ice. The ice shreds in places without being expulsed. This phenomenon could be due to a fragility and a lack of cohesion of the ice layer below a certain thickness. As a general rule, repeated sweeping allows to obtain at least a partial de-icing (>70 %) when the thickness is higher than 0.5 mm. A summary of the influence of the ice thickness is shown in Table 1 (tests 4, 6 to 8).

5.4 Mixed ice

The icing bench also allows to realize "mixed" ice with the interface layer being close to a glaze ice and the outer layers being more equivalent to rime ice. A few trials were carried out in order to test the effectiveness of the de-icing under these conditions. With an average deposit thickness of 2.2 mm, tests show an effective de-icing at the first repetition for the central zone of the ice. Detachment into large pieces is observed indicating de-icing mechanisms similar to glaze-type icing. In the second repetition, the thinner areas do not detach as patches but explode locally by de-icing localized "spots". For such ice layers the surface is de-iced by more

than 80 %. Another test, with a deposit of 1 mm, confirms this phenomenon of spot de-icing (see Figure 10) with a de-iced zone of a little more than 50 %. One hypothesis is the lack of cohesion of this type of ice, which does not allow for plate-like de-icing and which, as a result, is de-iced only locally. The de-icing efficiency on this type of ice is weaker with a need for many repetitions to increase the de-iced surface without however succeeding in a complete cleaning.

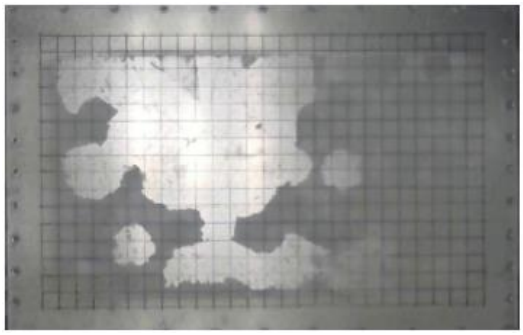

Figure 10: Experiments on mixed ice of thickness 1 mm. Local ice expulsion can be observed primarily around the location where the actuator is fixed to the aluminum plate.

6. Discussion

The de-icing system presented in this paper uses a compact piezoelectric actuator generating relatively high output displacements at compact size of 78 mm x 24 mm x 12 mm3 with a mass of 48 g. This actuator has been chosen with regard to a future integration into a leading edge. Extrapolated to a surface area to de-ice of 1 m2 (i.e. 28 actuators), a total mass of less than 1.5 kg would be applied to the airplane by this type of electromechanical de-icing. Various tests gave insight into the Eigen mode shapes and amplitudes to be reached for efficient de-icing on a flat rectangular aluminum plate. Exiting a single selected Eigen mode did not yield efficient de-icing. It is the fast transition between multiple mode shapes, which allows removing ice from the plate. Taken the voltage and current requirements from the Cedrat LA75C amplifier (maximum current output of 3 A) over the frequency range of 700 Hz to 3000 Hz for a 2 s sine sweep, the average apparent power at the operating amplitude (80 Vpp) is 41.5 W (see Figure 11). This gives about 1140 W/m2 when extrapolated from the iced surface dimension of 260 mm x 140 mm.

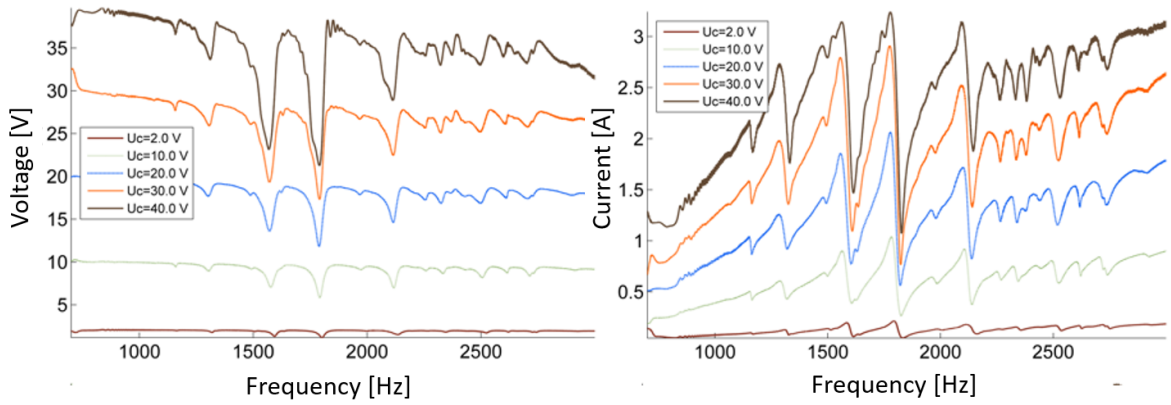

Figure 11: Voltage and current requirements of the APA400MML actuator powered with a Cedrat LA75C amplifier for a logarithmic sine sweep of 2 s and a frequency range between 700 Hz and 3000 Hz.

Table 1: Summary of de-icing tests.

Test number	Type of ice	Ice thickness [mm]	De-iced surface [%]	Frequency range [Hz]	Drive voltage [Vp]	De-icing sequence time	De-icing sequence repetitions	Instant power per m2 [W]	Average power per m2 [W]
1	Glaze	2	>95	4000-100	75	2	1	6180	-
2	Glaze	2	>90	4000-100	40	2	3	3300	1263
3	Glaze	1.2	>90	4000-700	40	2	3	3300	1373
4	Glaze	1.2	>95	3000-700	40	2	2	3300	1140
5	Glaze	1.2	>95	2100-1000	40	2	2	3300	961
6	Glaze	2	>95	3000-700	40	2	1	3300	1140
7	Glaze	0.8	>90	3000-700	40	2	3	3300	1140
8	Glaze	0.5	>50	3000-700	40	2	7	3300	1140
9	Mixed	2.2	>80	2100-1000	40	2	3	3300	961
10	Mixed	1	>50	2100-1000	40	2	4	3300	961

In order to give a first estimation of the modal behavior of a leading edge, a modal analysis of a NACA0012 profile made of aluminum with dimensions 300 x 200 x 1 mm3 has been carried out. The first 12 mode shapes are shown in Figure 12. The amplified piezoelectric actuator whose stiffness and mass is taken into account in this analysis is placed off-center in order to again protect the actuator from excessive vibration amplitudes. As expected, the Eigen frequencies are higher compared to the flat plate because of the curvature. Nevertheless, some mode shapes with convenient spatial frequency and at the desired frequency range can be found. Further studies need to be carried out to evaluate such a system.

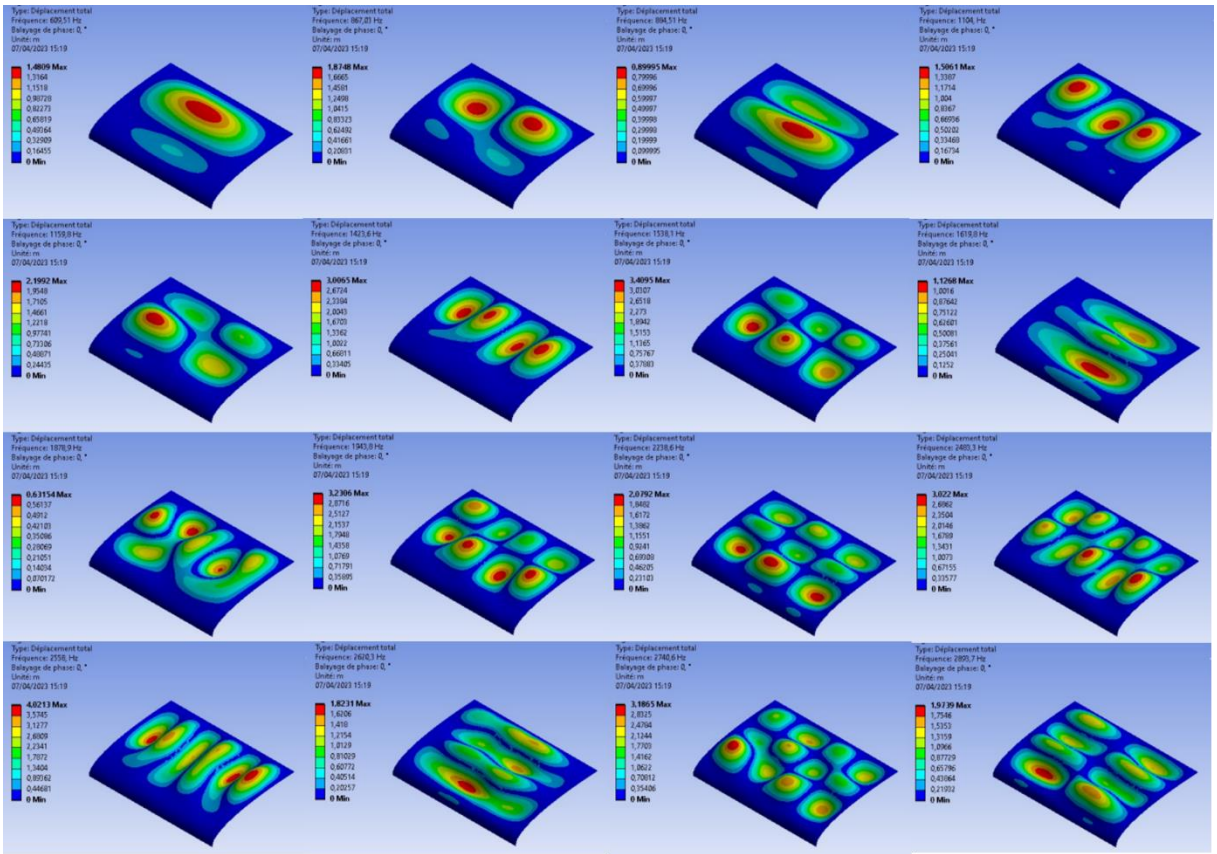

Figure 12: Simulated modal response of an aluminum NACA0012 profile of dimension 300 x 200 x 1 mm3.

7. Conclusion and future work

In this work, an electromechanical de-icing system incorporating an amplified piezoelectric actuator was presented. The actuator induces vibrations in the structure to de-ice and uses its Eigen modes to break the adhesive force between an ice layer and the aluminum structure. Various tests have been carried out changing the driving voltage, the frequency range, and the ice thickness in order to find the best-suited parameters. This parametric study allowed to better understand the phenomenon of modal electromechanical de-icing and in particular to neglect the excitation of high frequencies not necessary for de-icing. It has been shown that the combination of a short wavelength and a high amplitude is creating important stresses at the aluminum/ice interface leading to the detachment of the ice. Indeed, the use of modes of sufficient amplitude with wavelengths of the order of 80 mm shows a high efficiency for de-icing. Experiments showed that it is not necessary to have very low frequency and maximum amplitude modes on the spectrum to obtain a better de-icing efficiency. Numerous tests have confirmed a repeatable effect that can lead to a robust de-icing process. Although de-icing becomes difficult as the thickness of the ice layer decreases, it was possible to remove samples of the "glaze" type ice with a thickness greater than 1 mm without any problems. The tests carried out on a mixed ice showed a reduced efficiency but still possible with this approach.

Future work will include testing on a leading edge profile in order to test the efficiency of such a system on curved surfaces. Ideally, such tests should be carried out in a wind tunnel to simulate aerodynamic loading. Lower temperatures as can be found on aircrafts in the range of -30°C to -40°C could also be interesting to verify the ice-removal process.

8. Acknowledgement

This work has been carried out in collaboration with Zodiac Aerospace between 2012 and 2014.

9. References

[1] S. Venna et al., ”Piezoelectric transducer actuated leading edge de-icing with simultaneous shear and impulse forces,” Journal of Aircraft, Vol. 44, No. 2, 2007.

[2] S. V. Venna and Y.-J. Lin, "Mechatronic Development of Self-Actuating In-Flight Deicing Structures," in IEEE/ASME Transactions on Mechatronics, vol. 11, no. 5, pp. 585-592, Oct. 2006.

[3] E. Villeneuve, S. Ghinet, C. Volat, “Experimental Study of a Piezoelectric De-Icing System Implemented to Rotorcraft Blades,” Appl. Sci. 2021, 11, 9869.

[4] A. Overmeyer, J. Palacios, E. Smith, “Ultrasonic De-Icing Bondline Design and Rotor Ice Testing,” AIAA Journal. Vol. 51. Pp. 2965-2976, 2013.

[5] M. Kalkowski, T. Waters, E. Rustighi, “Removing surface accretions with piezo-excited high-frequency structural waves,” SPIE Smart Structures & NDE 2015.

[6] C. Laforte, « Déformation à la rupture adhésive par traction, flexion, et torsion d'un substrat givré°», PhD thesis, UNIVERSITÉ DU QUÉBEC À CHICOUTIMI, 2008.

[7] Caroline Laforte & Jean-Louis Laforte, Deicing Strains and Stresses of Iced Substrates, Journal of Adhesion Science and Technology, 26:4-5, 603-620, 2012.

[8] CEDRAT Technologies APA400MML; datasheet accessed on April 6th, 2023 ; https://www.cedrat-technologies.com/fileadmin/datasheets/APA400MML.pdf